

Polarimetric Scattering Decomposition Theorems

Carlos López-Martínez, Eric Pottier



1	Polarimetric Scattering Decomposition Theorems	2
1.1	Introduction	2
1.2	Coherent Scattering Decomposition Techniques.....	2
1.2.1	Introduction	2
1.2.2	The Pauli Decomposition	3
1.3	Incoherent Scattering Decomposition Techniques	5
1.3.1	Introduction	5
1.3.2	Three-Component Freeman Decomposition.....	6
1.3.3	Four-Component Yamaguchi Decomposition	10
1.3.4	Non-Negative Eigenvalue Decomposition.....	13
1.3.5	Eigenvector-Eigenvalue based Decomposition	17
1.3.6	The Touzi target scattering decomposition	21

1 Polarimetric Scattering Decomposition Theorems

1.1 Introduction

As shown previously, the scattering matrix or the covariance and coherency matrices allow the characterization of a scatterer for a given frequency and a given imaging geometry. The information provided by these matrices, at a particular combination of transmitting and receiving polarization states, can be extended to any polarization state thanks to the concept of polarization synthesis. Nevertheless, when facing real polarimetric SAR data, the interpretation of these matrices is not straightforward due to the complexity of the scattering process and the high variability of the scatterers. Polarimetric decomposition techniques appear as a solution to interpret the information provided by the scattering and the covariance and coherency matrices. These decomposition techniques must be divided into two main classes. The first one, referred to as *Coherent Polarimetric Decompositions* makes reference to those decomposition techniques applied to the scattering matrix. The validity of these decomposition techniques is restricted to point scatterers, that is, scatterers not affected by the speckle noise component. If applied to distributed scatterers, these decompositions would be random as they are not able to cope with the stochastic nature of the measurement. Distributed scatterers, on the contrary, can be analyzed by the so-called *Incoherent Polarimetric Decompositions* that base the analysis on the covariance or coherency matrices.

1.2 Coherent Scattering Decomposition Techniques

1.2.1 Introduction

The 2×2 complex scattering matrix is a mathematical operator able to describe the scattering process that occurs when a wave reaches a given scatterer. As indicated, this matrix contains the necessary information to determine the far-field scattered wave by the scatterer as a function of the incident wave. Consequently, the scattering matrix characterizes the scatterer, for the employed imaging geometry and the working frequency. As indicated previously, simple canonical scattering mechanisms may be recognized from the scattering matrix. Nevertheless, in real measurements, the scattering matrix usually presents a more complex structure that hinders the interpretation in physical terms. The objective behind coherent scattering decomposition techniques is to decompose the measured scattering matrix by the SAR system, i.e. \mathbf{S} , as a combination of the scattering matrices corresponding to simpler targets

$$\mathbf{S} = \sum_{i=1}^k c_i \mathbf{S}_i \quad (1.1)$$

In (1.1), the symbol \mathbf{S}_i corresponds to the response of every one of the simple or canonical scatterers, whereas the complex coefficients c_i indicate the weight of \mathbf{S}_i in the combination leading to the measured \mathbf{S} . As observed in (1.1), the term combination refers to the weighted addition of the k scattering matrices. In order to simplify the understanding of (1.1), but also, with the objective to make possible the decomposition itself, it is desirable that the matrices \mathbf{S}_i present the property of independence among them to avoid a particular scattering behavior to appear in more than one matrix \mathbf{S}_i . Often, the independence condition is substituted by the most restrictive property of orthogonality of the components \mathbf{S}_i . Orthogonality helps to eliminate possible ambiguities in the decomposition of the scattering matrix in those cases in which the elements \mathbf{S}_i are not orthogonal.

The scattering matrix \mathbf{S} characterizes the scattering process produced by a given scatterer, and therefore the scatterer itself. This is possible only in those cases in which both, the incident and the scattered waves are completely polarized waves. Consequently, coherent scattering decompositions can be only employed to study the so-called coherent scatterers. These scatterers are also known as point or pure targets.

In a real situation, the measured scattering matrix by the radar \mathbf{S} corresponds to a complex coherent scatterer. Only in some occasions, this matrix will correspond to a simpler or canonical object, which a good example is, for instance, the trihedrals employed to calibrate SAR imagery. In a general situation, a direct analysis of the matrix \mathbf{S} , with the objective to infer the physical properties of the scatterer under study, is shown to be complex. Consequently, the physical properties of the target under study are extracted and interpreted through the analysis of the simpler responses \mathbf{S}_i and the corresponding complex coefficients C_i in (1.1).

The decomposition exposed in (1.1) is not unique in the sense that it is possible to find a number of infinite sets $\{\mathbf{S}_i; i = 1, \dots, k\}$ in which the matrix \mathbf{S} can be decomposed. Nevertheless, only some of the sets $\{\mathbf{S}_i; i = 1, \dots, k\}$ are convenient in order to interpret the information contained in \mathbf{S} . Two examples of these decomposition bases have been already shown previously. Other examples of coherent scattering decompositions are the *Krogager* [R82][R83][R84] or the *Cameron decompositions* [R85][R86].

1.2.2 The Pauli Decomposition

The most relevant coherent scattering decomposition is the *Pauli decomposition*, which expresses the measured scattering matrix \mathbf{S} in the so-called Pauli basis. If we considered the conventional orthogonal linear basis $\{\hat{h}, \hat{v}\}$, in a general case, the Pauli basis $\{\mathbf{S}_a, \mathbf{S}_b, \mathbf{S}_c, \mathbf{S}_d\}$ is given by the following four 2×2 matrices

$$\mathbf{S}_a = \frac{1}{\sqrt{2}} \begin{bmatrix} 1 & 0 \\ 0 & 1 \end{bmatrix} \quad (1.2)$$

$$\mathbf{S}_b = \frac{1}{\sqrt{2}} \begin{bmatrix} 1 & 0 \\ 0 & -1 \end{bmatrix} \quad (1.3)$$

$$\mathbf{S}_c = \frac{1}{\sqrt{2}} \begin{bmatrix} 0 & 1 \\ 1 & 0 \end{bmatrix} \quad (1.4)$$

$$\mathbf{S}_d = \frac{1}{\sqrt{2}} \begin{bmatrix} 0 & -1 \\ 1 & 0 \end{bmatrix} \quad (1.5)$$

As mentioned, it has been always considered that $S_{hv} = S_{vh}$, since reciprocity applies in a monostatic system configuration under the BSA convention. In this situation, the Pauli basis can be reduced to a basis composed by the matrices (1.2), (1.3) and (1.4), that is, $\{\mathbf{S}_a, \mathbf{S}_b, \mathbf{S}_c\}$. Consequently, given a measured scattering matrix \mathbf{S} , this matrix can be expressed as follows

$$\mathbf{S} = \begin{bmatrix} S_{hh} & S_{hv} \\ S_{hv} & S_{vv} \end{bmatrix} = a\mathbf{S}_a + b\mathbf{S}_b + c\mathbf{S}_c \quad (1.6)$$

where the complex coefficients that determine the contribution of every component of the basis can be obtained as

$$a = \frac{S_{hh} + S_{vv}}{\sqrt{2}} \quad (1.7)$$

$$b = \frac{S_{hh} - S_{vv}}{\sqrt{2}} \quad (1.8)$$

$$c = \sqrt{2} S_{hv} \quad (1.9)$$

From the previous equations, it can be shown that

$$SPAN(\mathbf{S}) = |S_{hh}|^2 + |S_{vv}|^2 + 2|S_{hv}|^2 = |a|^2 + |b|^2 + |c|^2 \quad (1.10)$$

The interpretation of the Pauli decomposition must be done according to the matrices $\{\mathbf{S}_a, \mathbf{S}_b, \mathbf{S}_c\}$ and their corresponding decomposition coefficients, i.e., $\{a, b, c\}$. Previously it was seen that the matrices $\{\mathbf{S}_a, \mathbf{S}_b, \mathbf{S}_c\}$ correspond to the scattering behavior of some canonical bodies.

- The matrix \mathbf{S}_a corresponds to the scattering matrix of a sphere, a plate or a trihedral. Generally, \mathbf{S}_a is referred to as single- or odd-bounce scattering. Hence, the complex coefficient a represents the contribution of \mathbf{S}_a to the final measured scattering matrix. In particular, the intensity of this coefficient, i.e., $|a|^2$, determines the power scattered by scatterers characterized by single- or odd-bounce.
- The matrix, \mathbf{S}_b , represents the scattering mechanism of a dihedral oriented at 0 degrees. In general, this component indicates a scattering mechanism characterized by double- or even-bounce, since the polarization of the returned wave is mirrored respect to the one of the incident wave. Consequently, b stands for the complex coefficient of this scattering mechanism and $|b|^2$ represents the scattered power by this type of targets.
- The matrix \mathbf{S}_c corresponds to the scattering mechanism of a diplane oriented at 45 degrees. As it can be observed in (1.4), and considering that this matrix is expressed in the linear orthogonal basis $\{\hat{\mathbf{h}}, \hat{\mathbf{v}}\}$, the scatterer returns a wave with a polarization orthogonal to the one of the incident wave. From a qualitative point of view, the scattering mechanism represented by \mathbf{S}_c is referred to those scatterers which are able to return the orthogonal polarization, from which, one of the best examples is the volume scattering produced by the forest canopy. The complex scattering that occurs in the forest canopy, characterized by multiple reflections, makes possible to return energy on the orthogonal polarization, respect to the polarization of the incident wave. Consequently, this third scattering mechanism is usually referred to as volume scattering. The coefficient c represents the contribution of \mathbf{S}_c to \mathbf{S} , whereas $|c|^2$ stands for the scattered power by this type of scatters.

The Pauli decomposition of the scattering matrix is often employed to represent the polarimetric information in a single SAR image. The polarimetric information of \mathbf{S} could be represented with the combination of the intensities $|\mathbf{S}_{hh}|^2$, $|\mathbf{S}_{vv}|^2$ and $2|\mathbf{S}_{hv}|^2$ in a single RGB image, i.e., every of the previous intensities coded as a color channel. The main drawback of this approach is the physical interpretation of the resulting image in terms of $|\mathbf{S}_{hh}|^2$, $|\mathbf{S}_{vv}|^2$ and

$2|S_{hv}|^2$. Consequently, a RGB image can be created with the intensities $|a|^2$, $|b|^2$ and $|c|^2$, which, as indicated previously, correspond to clear physical scattering mechanisms. Thus, the resulting colour image can be employed to interpret the physical information from a qualitative point of view. The most employed codification corresponds to

$$|a|^2 \rightarrow \text{Blue}, |b|^2 \rightarrow \text{Red}, |c|^2 \rightarrow \text{Green} \quad (1.11)$$

Then, the resulting colour of the RGB image is interpreted in terms of scattering mechanism as given by (1.2), (1.3) and (1.4).

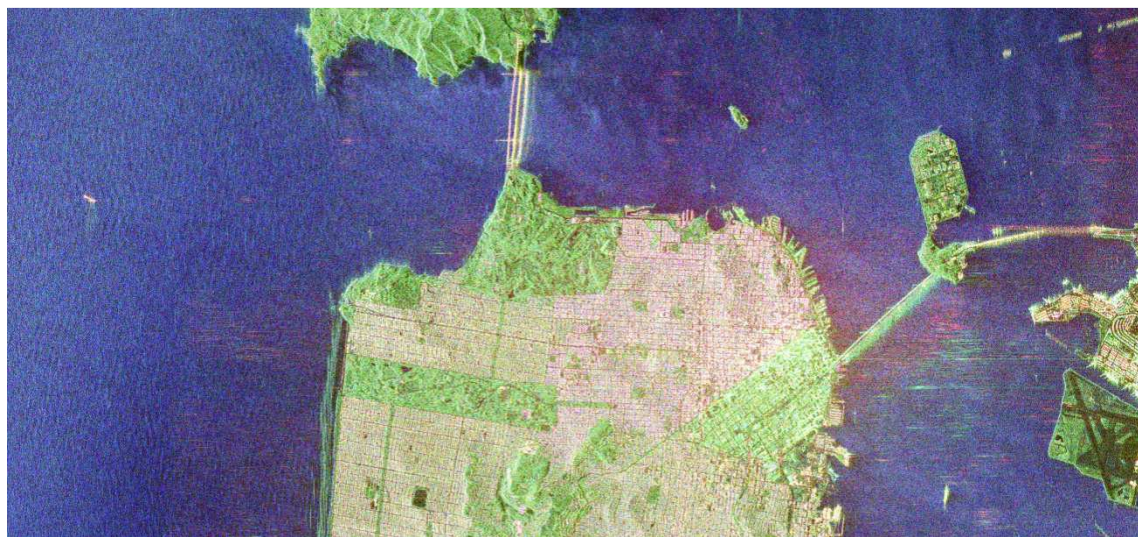


Figure 1.1 – Radarsat-2 polarimetric RGB-Pauli image over San Francisco (USA) where the colour code is: $|S_{hh} + S_{vv}|^2$ blue, $|S_{hh} - S_{vv}|^2$ red and $2|S_{hv}|^2$ green.

1.3 Incoherent Scattering Decomposition Techniques

1.3.1 Introduction

As explained in the previous sections, the scattering matrix \mathbf{S} is only able to characterize the point or deterministic scatterers. In this case, the scattering process is completely determined by the five independent parameters the matrix \mathbf{S} may present. On the contrary, this matrix cannot be employed to characterize, from a polarimetric point of view, the distributed scatterers, as the five independent parameters of the \mathbf{S} matrix are insufficient to characterize the scattering process. As detailed previously, distributed scatterers can be only characterized statistically due to the presence of speckle noise by means of higher order descriptors. Since speckle noise must be reduced, only second order polarimetric representations can be employed to analyze distributed scatterers. In the case of monostatic scattering under the BSA convention, these second order descriptors are the 3×3 , Hermitian covariance \mathbf{C} or coherency \mathbf{T} matrices.

The complexity of the scattering process makes extremely difficult the physical study of a given scatterer through the direct analysis of \mathbf{C} or \mathbf{T} . Hence, the objective of the incoherent decompositions is to separate the \mathbf{C} or \mathbf{T} matrices as the combination of second order descriptors corresponding to simpler or canonical objects, presenting an easier physical interpretation. These decomposition theorems can be expressed as

$$\mathbf{C} = \sum_{i=1}^k p_i \mathbf{C}_i \quad (1.12)$$

$$\mathbf{T} = \sum_{i=1}^k q_i \mathbf{T}_i \quad (1.13)$$

where the canonical responses are represented by \mathbf{C}_i and \mathbf{T}_i , and p_i and q_i denote the coefficients of these components in \mathbf{C} or \mathbf{T} , respectively. As in the case of the coherent decompositions, it is desirable that these components present some properties. First of all, it is desirable that the components \mathbf{C}_i and \mathbf{T}_i correspond to pure scatterers in order to simplify the physical study. Nevertheless, this condition is not absolutely necessary and \mathbf{C}_i and \mathbf{T}_i may also represent distributed scatterers. In addition, the components \mathbf{C}_i and \mathbf{T}_i should be independent, or in a more restrictive way, orthogonal.

The bases in which \mathbf{C} or \mathbf{T} are decomposed, i.e., $\{\mathbf{C}_i; i=1, \dots, k\}$ and $\{\mathbf{T}_i; i=1, \dots, k\}$ are not unique. Consequently, these different bases give rise to different incoherent scattering decomposition techniques.

1.3.2 Three-Component Freeman Decomposition

The *Freeman decomposition*, also known as *Freeman-Durden decomposition* [R87], is the best exponent of the so-called *model based decompositions*. In this type of decompositions, the canonical scattering mechanisms \mathbf{C}_i and \mathbf{T}_i in which the original matrices are decomposed into are fixed by the decomposition itself, i.e., the scattering mechanisms are imposed. The main drawback of this approach is that the decomposition technique will try to find these mechanisms, even though these are not present in the original matrices. In particular, the Freeman decomposition decomposes the original covariance or coherency matrices into the three following scattering mechanisms:

- *Volume scattering*, where a canopy scatterer is modelled as a set of randomly oriented dipoles.
- *Double-bounce scattering*, modelled as a dihedral corner reflector.
- *Surface or single-bounce scattering*, modelled as a first-order Bragg surface scatter.

In the following, and without lack of generality, a formulation in terms if the covariance matrix \mathbf{C} is considered.

The volume scattering component, mainly considered in forested areas, is modeled as the contribution from an ensemble of randomly oriented thin dipoles. The scattering matrix of an elementary dipole, expressed in the orthogonal linear basis $\{\hat{\mathbf{h}}, \hat{\mathbf{v}}\}$, when horizontally oriented, presents the expression

$$\mathbf{S} = \begin{bmatrix} S_{hh} & 0 \\ 0 & S_{vv} \end{bmatrix} \quad (1.14)$$

For a thin dipole, the previous scattering matrix reduces to

$$\mathbf{S} = \begin{bmatrix} 1 & 0 \\ 0 & 0 \end{bmatrix} \quad (1.15)$$

Now, if a set of randomly oriented dipoles, characterized by the previous scattering matrix and oriented according to a uniform phase distribution is considered, the covariance matrix of the ensemble of thin dipoles corresponds to the following covariance matrix

$$\mathbf{C}_v = \frac{f_v}{8} \begin{bmatrix} 3 & 0 & 1 \\ 0 & 2 & 0 \\ 3 & 0 & 3 \end{bmatrix} \quad (1.16)$$

where f_v corresponds to the contribution of the volume scattering. The covariance matrix \mathbf{C}_v presents a rank equal to three. Thus, the volume scattering cannot be characterized by a single scattering matrix of a pure scatterer. Finally, it is worth to indicate, as observed in (1.16), that the model assumed for forest scattering in the Freeman decomposition is fixed. In contrast, the other two scattering components of the decomposition, as it will be shown, admit a higher degree of flexibility.

The second component of the Freeman decomposition corresponds to double-bounce scattering. In this case, a generalized corner reflector is employed to model this scattering process. The diplane itself is not considered metallic. Hence, it is assumed that the vertical surface presents reflection coefficients R_{th} and R_{tv} for the horizontal and the vertical polarizations, respectively, whereas the horizontal surface presents the coefficients R_{gh} and R_{gv} for the same polarizations. Additionally, two phase components for the horizontal and the vertical polarizations are considered, i.e., $e^{j2\gamma_h}$ and $e^{j2\gamma_v}$, respectively. The complex phase constants γ_h and γ_v account for any attenuation or phase change effect. Hence, the scattering matrix of this generalized dihedral corresponds to

$$\mathbf{S} = \begin{bmatrix} e^{j2\gamma_h} R_{gh} R_{th} & 0 \\ 0 & e^{j2\gamma_v} R_{gv} R_{tv} \end{bmatrix} \quad (1.17)$$

which gives rise to the covariance matrix of the double-bounce scattering component. After normalization respect to the \mathbf{S}_{vv} component, this covariance matrix can be written as follows

$$\mathbf{C}_d = f_d \begin{bmatrix} |\alpha|^2 & 0 & \alpha \\ 0 & 0 & 0 \\ \alpha^* & 0 & 1 \end{bmatrix} \quad (1.18)$$

where

$$\alpha = e^{j2(\gamma_h - \gamma_v)} \frac{R_{gh} R_{th}}{R_{gv} R_{tv}} \quad (1.19)$$

and f_d corresponds to the contribution of the double-bounce scattering to the $|\mathbf{S}_{vv}|^2$ component

$$f_d = |R_{gv} R_{tv}|^2 \quad (1.20)$$

As it can be observed, in this case the covariance matrix \mathbf{C}_d presents a rank equal to 1, and therefore it may be represented by the scattering matrix given by (1.17).

The third component of the Freeman decomposition consists of a first-order Bragg surface scattering modelling a surface rough scattering. The scattering mechanism is represented by the following scattering matrix

$$\mathbf{S} = \begin{bmatrix} R_h & 0 \\ 0 & R_v \end{bmatrix} \quad (1.21)$$

where R_h and R_v denote the reflection coefficients for horizontally and vertically polarized waves, respectively. Consequently, the covariance matrix corresponding to this scattering component is

$$\mathbf{C}_s = f_s \begin{bmatrix} |\beta|^2 & 0 & \beta \\ 0 & 0 & 0 \\ \beta^* & 0 & 1 \end{bmatrix} \quad (1.22)$$

where f_s corresponds to the contribution of the double-bounce scattering to the $|\mathbf{S}_{vv}|^2$ component

$$f_s = |R_v|^2 \quad (1.23)$$

$$\beta = \frac{R_h}{R_v} \quad (1.24)$$

As in the case for the double-bounce scattering mechanism, since the matrix \mathbf{C}_s presents a rank equal to 1, the scattering process is completely represented by the scattering mechanism presented previously.

Finally, it can be seen that the Freeman decomposition expresses the measured covariance matrix \mathbf{C} as

$$\mathbf{C} = \mathbf{C}_v + \mathbf{C}_d + \mathbf{C}_s \quad (1.25)$$

that takes the expression

$$\mathbf{C} = \begin{bmatrix} \frac{3f_v}{8} + f_d |\alpha|^2 + f_s |\beta|^2 & 0 & \frac{f_v}{8} + f_d \alpha + f_s \beta \\ 0 & \frac{2f_v}{8} & 0 \\ \frac{f_v}{8} + f_d \alpha^* + f_s \beta^* & 0 & \frac{3f_v}{8} + f_d + f_s \end{bmatrix} \quad (1.26)$$

As one may deduce from (1.26), the Freeman decomposition presents 5 independent parameters $\{f_v, f_d, f_s, \alpha, \beta\}$ but only 4 equations. Consequently, some hypothesis must be considered in order to find the values of $\{f_v, f_d, f_s, \alpha, \beta\}$.

Considering that the Span of the covariance matrix may be expressed as a function of the power scattered by each component of the decomposition $\{\mathbf{C}_v, \mathbf{C}_d, \mathbf{C}_s\}$, i.e.,

$$SPAN(\mathbf{C}) = |S_{hh}|^2 + |S_{vv}|^2 + 2|S_{hv}|^2 = P_v + P_d + P_s \quad (1.27)$$

the term P_v corresponds to the contribution of the volume scattering of the final covariance matrix \mathbf{C} . Hence, the scattered power by this component may be written as

$$P_v = f_v \quad (1.28)$$

The power scattered by the double-bounce component is expressed as

$$P_d = f_d (1 + |\alpha|^2) \quad (1.29)$$

whereas the power scattered by the surface component is

$$P_s = f_s (1 + |\beta|^2) \quad (1.30)$$

Consequently, the scattered power at each component $\{P_v, P_d, P_s\}$ may be employed to generate a RGB image, similarly as in the case of the Pauli decomposition, to present all the colour-coded polarimetric information in a unique image, see Figure 1.2.

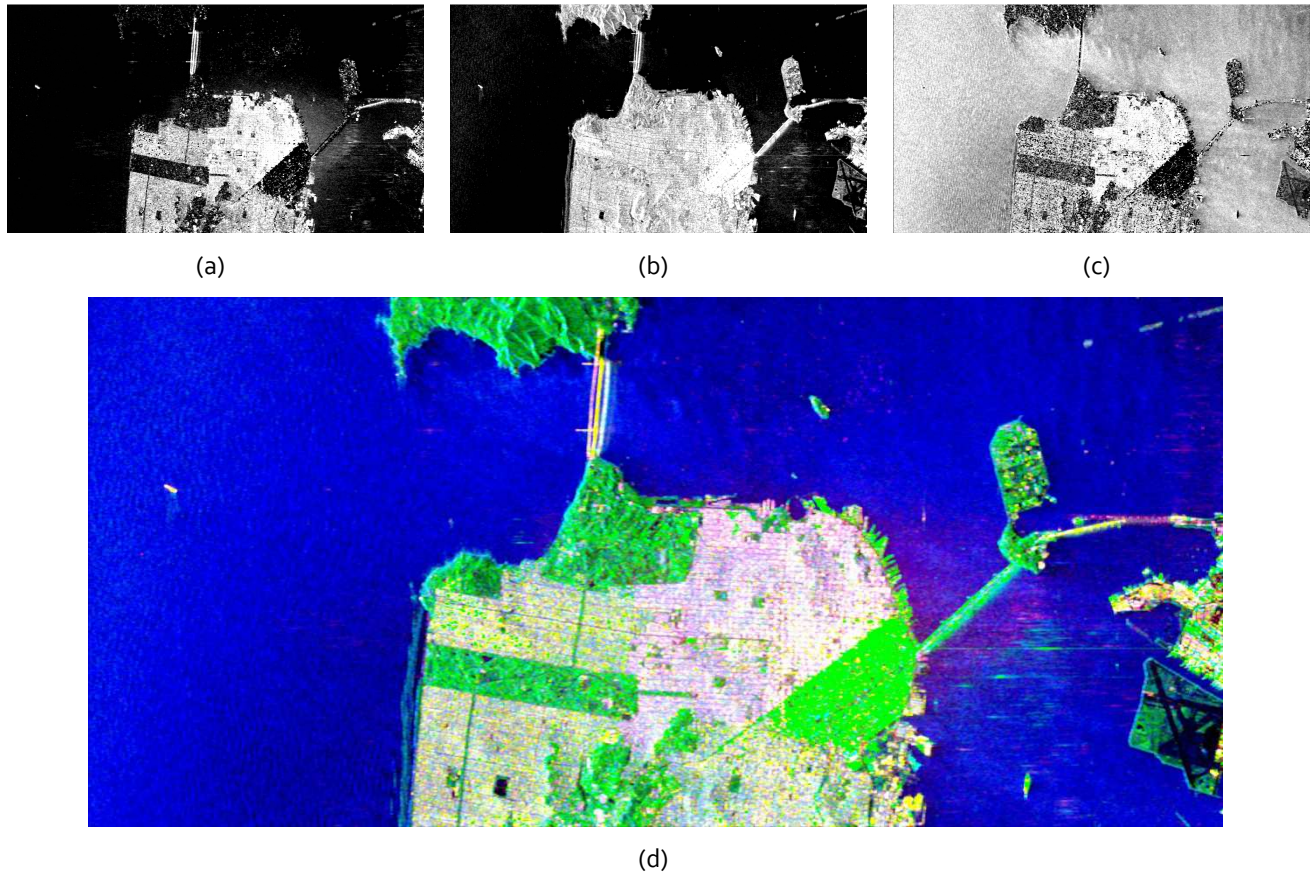


Figure 1.2 – Freeman decomposition of the Radarsat-2 polarimetric RGB-Pauli image over San Francisco (USA). (a) P_d , (b) P_v , (c) P_s , (d) RGB composition where P_d red, P_v green and P_s blue.

1.3.3 Four-Component Yamaguchi Decomposition

As it may be observed in (1.26), the three-component Freeman decomposition is based on the assumption that the analyzed scatterer presents reflection symmetry, that is, the correlation of the copolar channels, either \mathbf{S}_{hh} or \mathbf{S}_{vv} , with the cross-polar one \mathbf{S}_{hv} is zero, that is $\langle S_{hh} S_{hv}^* \rangle = 0$ and $\langle S_{hv} S_{vv}^* \rangle = 0$. This type of symmetry in the scattering process appears normally in the case of natural distributed scatterers such forests or grassland areas. Nevertheless, in the case of more complex scattering scenarios, as for instance man-made scatterers, this assumption is no longer true. In addition to the previous limitation, the Freeman decomposition, as detailed in the previous section, considers only one type of volume scattering, as reflected in (1.16), where the scattering at the copolar channels are supposed equal, i.e., $\langle |S_{hh}|^2 \rangle = \langle |S_{vv}|^2 \rangle$. The *four-component Yamaguchi decomposition* is proposed to overcome the previous two limitations of the Freeman decomposition [R88][R89]. Consequently, this new decomposition could be understood as an evolution of the Freeman decomposition.

In one considers the canonical scattering mechanisms presented previously, it may be observed that only the rotated thin cylinder or the right and left handed helices are able to produce a covariance matrix such that $\langle S_{hh} S_{hv}^* \rangle \neq 0$ and $\langle S_{hv} S_{vv}^* \rangle \neq 0$, and therefore produce a covariance matrix without reflection symmetry. In the four-component Yamaguchi decomposition the authors propose to take into account the absence of this type of symmetry by considering first, the three scattering mechanisms considered by the Freeman decomposition, that is, volume, double-bounce and surface scattering, together with a fourth component composed by either the left or the right handed helix scattering [R82][R83][R84]. In particular, the helix scattering is characterized by generating a left-handed or a right-handed circular polarization for all incident linear polarizations, according to the scatterer helicity. The left hand helix, which scattering matrix presented previously, leads to the following covariance matrix

$$\mathbf{C}_{lh} = \frac{f_c}{4} \begin{bmatrix} 1 & -j\sqrt{2} & -1 \\ j\sqrt{2} & 2 & -j\sqrt{2} \\ -1 & j\sqrt{2} & 1 \end{bmatrix} \quad (1.31)$$

whereas the right hand helix results into the following covariance matrix

$$\mathbf{C}_{rh} = \frac{f_c}{4} \begin{bmatrix} 1 & j\sqrt{2} & -1 \\ -j\sqrt{2} & 2 & j\sqrt{2} \\ -1 & -j\sqrt{2} & 1 \end{bmatrix} \quad (1.32)$$

where f_c accounts for the contribution of the helix component. As it may be observed in the previous two matrices, the inclusion of the helix component allows to consider a scattering mechanism without reflection symmetry. The selection of the left or the right hand helix will be determined by the sign of the imaginary part of $\langle S_{hh} S_{hv}^* \rangle$ or $\langle S_{hv} S_{vv}^* \rangle$.

In order to model the volume scattering, the Freeman decomposition considered a set of randomly oriented dipoles, characterized by (1.15) and oriented according to a uniform phase distribution. Nevertheless, when confronted to a real forest, the effect of the trunk and the branches, especially at high frequencies, may lead to a scattering from a cloud of oriented dipoles but with a nonuniform distribution. In this case, depending on the main orientation of these thin dipoles, the power associated to $\langle |S_{hh}|^2 \rangle$ and $\langle |S_{vv}|^2 \rangle$ may be different if the dipoles are preferably oriented horizontally or vertically, respectively. As it may be seen, the volume model considered by the Freeman decomposition

(1.16) cannot take into account this effect. In order to account for this preference in the orientation, instead of considering a uniform distribution for the orientation of the thin dipoles, it is proposed to consider the following distribution

$$p(\theta) = \begin{cases} \frac{1}{2} \cos \theta & \text{for } |\theta| < \pi/2 \\ 0 & \text{for } |\theta| > \pi/2 \end{cases} \quad (1.33)$$

where θ is taken from the horizontal axis seen from the radar. When considering a cloud of randomly oriented, very thin horizontal dipoles, the volume scattering is represented by the following scattering matrix

$$\mathbf{C}_v = \frac{f_v}{15} \begin{bmatrix} 8 & 0 & 2 \\ 0 & 4 & 0 \\ 2 & 0 & 3 \end{bmatrix} \quad (1.34)$$

Otherwise, if the cloud of thin dipoles is considered to be formed by vertical dipoles, the covariance matrix representing the volume component is

$$\mathbf{C}_v = \frac{f_v}{15} \begin{bmatrix} 3 & 0 & 2 \\ 0 & 4 & 0 \\ 2 & 0 & 8 \end{bmatrix} \quad (1.35)$$

In all the cases, f_v corresponds to the contribution of the volume scattering.

Allowing the volume scattering to depend on the main orientation of the particles makes it necessary to introduce an additional step in the decomposition able to select the volume scattering most adapted to the data under observation. The four-component Yamaguchi decomposition proposes to select among (1.16), (1.34) and (1.35) according to the ratio $10\log\left(\langle |S_{vv}|^2 \rangle / \langle |S_{hh}|^2 \rangle\right)$. Table 1.1 details the procedure to select the type of volume scattering proposed in [R88].

$10\log\left(\langle S_{vv} ^2 \rangle / \langle S_{hh} ^2 \rangle\right) < -2 \text{ dB}$	$-2 \text{ dB} < 10\log\left(\langle S_{vv} ^2 \rangle / \langle S_{hh} ^2 \rangle\right) < 2 \text{ dB}$	$2 \text{ dB} < 10\log\left(\langle S_{vv} ^2 \rangle / \langle S_{hh} ^2 \rangle\right)$
$\mathbf{C}_v = \frac{f_v}{15} \begin{bmatrix} 8 & 0 & 2 \\ 0 & 4 & 0 \\ 2 & 0 & 3 \end{bmatrix}$	$\mathbf{C}_v = \frac{f_v}{8} \begin{bmatrix} 3 & 0 & 1 \\ 0 & 2 & 0 \\ 3 & 0 & 3 \end{bmatrix}$	$\mathbf{C}_v = \frac{f_v}{15} \begin{bmatrix} 3 & 0 & 2 \\ 0 & 4 & 0 \\ 2 & 0 & 8 \end{bmatrix}$

Table 1.1 – Selection of the volume scattering covariance matrix.

Finally, the double-bounce and the surface scattering components of the four-component Yamaguchi decomposition are the same as the Freeman decomposition. Consequently, the Yamaguchi decomposition models the covariance matrix as

$$\mathbf{C} = \begin{bmatrix} \frac{f_c}{4} + f_d |\alpha|^2 + f_s |\beta|^2 & \pm j \frac{\sqrt{2} f_c}{4} & -\frac{f_c}{4} + f_d \alpha + f_s \beta \\ \mp j \frac{\sqrt{2} f_c}{4} & \frac{f_c}{2} & \pm j \frac{\sqrt{2} f_c}{4} \\ -\frac{f_c}{4} + f_d \alpha^* + f_s \beta^* & \mp j \frac{\sqrt{2} f_c}{4} & \frac{f_c}{4} + f_d + f_s \end{bmatrix} + f_v \begin{bmatrix} a & 0 & d \\ 0 & b & 0 \\ d & 0 & c \end{bmatrix} \quad (1.36)$$

where the last matrix accounts for the volume scattering that has been selected according to Table 1.1. As one may deduce from (1.36), the four-component Yamaguchi decomposition presents 6 independent parameters $\{f_v, f_d, f_s, f_c, \alpha, \beta\}$.

Considering that the Span of the covariance matrix may be expressed as a function of the power scattered by each component of the decomposition $\{\mathbf{C}_v, \mathbf{C}_d, \mathbf{C}_s, \mathbf{C}_{lh/rh}\}$, i.e.,

$$SPAN(\mathbf{C}) = |S_{hh}|^2 + |S_{vv}|^2 + 2|S_{hv}|^2 = P_v + P_d + P_s + P_c \quad (1.37)$$

the term P_v corresponds to the contribution of the volume scattering of the final covariance matrix \mathbf{C} . Hence, the scattered power by this component may be written as

$$P_v = f_v \quad (1.38)$$

The power scattered by the double-bounce component is expressed as

$$P_d = f_d (1 + |\alpha|^2) \quad (1.39)$$

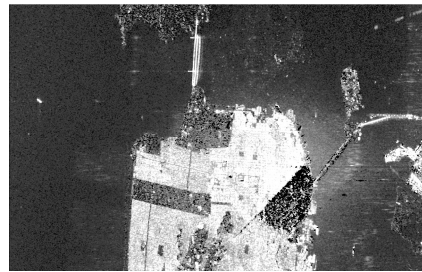
the power scattered by the surface component is

$$P_s = f_s (1 + |\beta|^2) \quad (1.40)$$

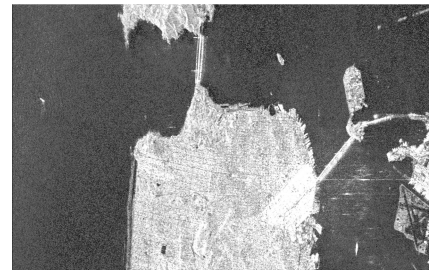
Whereas the power scattered by the helix component is

$$P_c = f_c \quad (1.41)$$

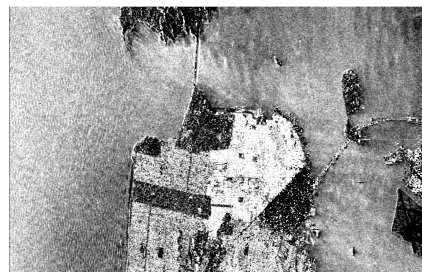
Consequently, the scattered power at each component $\{P_v, P_d, P_s, P_c\}$ may be combined to generate a RGB image similarly as in the case of the Pauli decomposition, to present all the colour-coded polarimetric information in a unique image, see Figure 1.3.



(a)



(b)



(c)



(d)



(e)

Figure 1.3 – Yamaguchi decomposition of the Radarsat-2 polarimetric RGB-Pauli image over San Francisco (USA). (a) P_d , (b) P_v , (c) P_s , (d) P_c , (e) RGB composition where P_d red, P_v green and P_s blue.

1.3.4 Non-Negative Eigenvalue Decomposition

As indicated in the previous two sections both, the Freeman-Durden, as well as the Yamaguchi decomposition work under the hypothesis that the measured covariance matrix may be decomposed as the sum of a set of scattering mechanisms. Whereas the first decomposition assumes reflection symmetry for the scattering medium, this limitation is addressed by the second one by considering a fourth scattering component represented by either the left or the right handed helix scattering. All the scattering mechanisms in which the measured covariance matrix is decomposed into are represented by their corresponding covariance matrices. As shown in [Rgo], these matrices should correspond to physical scattering mechanisms so all their eigenvalues must be larger than or equal to zero, in other words, the power received by any combination of transmitting and receiving polarizations should never be negative.

A close analysis of the Freeman-decomposition shows that the contribution of the volume scattering component is directly estimated from the cross-polarized term, that is, the decomposition assumes that neither the double-bounce nor the surface scattering components contribute to it. This assumption is very strict as, for instance, the rotation of the polarization basis of the scattering matrix due to terrain slopes in the along-track dimension [R91] or even rough surfaces may lead to significant cross-polarized power [R92]. Consequently, if these effects are not taken into account, they may produce an overestimation of the volume component. Once this volume component is estimated from the data, it is extracted from the measured covariance matrix to estimate the double-bounce and the surface components as

$$\mathbf{C}_{d+s} = \mathbf{C} - \mathbf{C}_v \quad (1.42)$$

Consequently, if the volume component is not properly estimated, the previous subtraction may lead to a result in which the covariance matrix representing the double-bounce and the surface components \mathbf{C}_{d+s} may present negative eigenvalues so it does not represent a physically possible scattering mechanism. The Yamaguchi decomposition also presents this drawback as the double-bounce and the surface like scattering components are estimated after the subtraction of the volume scattering component.

In order to correct the presence of negative eigenvalues when considering a decomposition based on (1.42), *van Zyl et al.* [R90] proposed the *Non-Negative Eigenvalue Decomposition* (NNED). The Freeman-Durden and the Yamaguchi decompositions assume that the measured covariance matrix results from the addition of a set of scattering mechanisms. Nevertheless, the NNED approach proposed to decompose the measured covariance matrix as

$$\mathbf{C} = a\mathbf{C}_{\text{model}} + \mathbf{C}_{\text{remainder}} \quad (1.43)$$

The matrix $\mathbf{C}_{\text{model}}$ represents the covariance matrix predicted by a theoretical model, as for instance, the volume scattering component. The parameter a is introduced in (1.43) to assure that all the matrices in (1.43) represent physically realizable scattering mechanism. Finally, the second matrix $\mathbf{C}_{\text{remainder}}$ will contain whatever is in the measured matrix \mathbf{C} that is not consistent with the model matrix $\mathbf{C}_{\text{model}}$.

To find the value of a , (1.43) may be written as

$$\mathbf{C}_{\text{remainder}} = \mathbf{C} - a\mathbf{C}_{\text{model}} \quad (1.44)$$

Consequently, the value of a must assure that the eigenvalues of $\mathbf{C}_{\text{remainder}}$ must be positive. In the case of a scattering media with reflection symmetry, (1.43) may be written as

$$\mathbf{C}_{\text{remainder}} = \begin{bmatrix} \xi & 0 & \rho \\ 0 & \eta & 0 \\ \rho^* & 0 & \zeta \end{bmatrix} - a \begin{bmatrix} \xi_a & 0 & \rho_a \\ 0 & \eta_a & 0 \\ \rho_a^* & 0 & \zeta_a \end{bmatrix} \quad (1.45)$$

Therefore, the maximum value of a that assures that the eigenvalues of $\mathbf{C}_{\text{remainder}}$ are positive corresponds to

$$a_{\max} = \min \left\{ \frac{\eta/\eta_a}{2(\xi_a \zeta_a - |\rho_a|^2)}, \frac{1}{2(\xi_a \zeta_a - |\rho_a|^2)} \left\{ Z - \sqrt{Z^2 - 4(\xi_a \zeta_a - |\rho_a|^2) \xi \zeta - |\rho|^2} \right\} \right\} \quad (1.46)$$

where $Z = (\xi \zeta_a + \zeta \xi_a) - \rho \rho_a^* - \rho^* \rho_a$. For the case of scattering media not presenting reflection symmetry, the process to derive the maximum value of a is similar, but resulting into more complex expressions.

The volume scattering model employed for the canopy scattering is based on a cosine-squared distribution raised to the n th power for the vegetation orientation [R93]. Considering that the basic scatterer in the canopy is a dipole, it was shown that the covariance matrix can be written as

$$\mathbf{C}_v(\theta_0, \sigma) = \mathbf{C}_\alpha + p(\sigma)\mathbf{C}_\beta + q(\sigma)\mathbf{C}_\gamma \quad (1.47)$$

where

$$\mathbf{C}_\alpha = \frac{1}{8} \begin{bmatrix} 3 & 0 & 1 \\ 0 & 2 & 0 \\ 3 & 0 & 3 \end{bmatrix} \quad (1.48)$$

$$\mathbf{C}_\beta = \frac{1}{8} \begin{bmatrix} -2\cos 2\theta_0 & \sqrt{2}\cos 2\theta_0 & 0 \\ \sqrt{2}\cos 2\theta_0 & 0 & \sqrt{2}\cos 2\theta_0 \\ 0 & \sqrt{2}\cos 2\theta_0 & 2\cos 2\theta_0 \end{bmatrix} \quad (1.49)$$

$$\mathbf{C}_\gamma = \frac{1}{8} \begin{bmatrix} \cos 4\theta_0 & -\sqrt{2}\cos 4\theta_0 & -\cos 4\theta_0 \\ -\sqrt{2}\cos 4\theta_0 & -2\cos 4\theta_0 & \sqrt{2}\cos 4\theta_0 \\ -\cos 4\theta_0 & \sqrt{2}\cos 4\theta_0 & \cos 4\theta_0 \end{bmatrix} \quad (1.50)$$

and

$$p(\sigma) = 2.0806\sigma^6 - 6.3350\sigma^5 + 6.3864\sigma^4 - 0.4431\sigma^3 - 3.9638\sigma^2 - 0.0008\sigma + 2.000 \quad (1.51)$$

$$q(\sigma) = 9.0166\sigma^6 - 18.7790\sigma^5 + 4.9590\sigma^4 + 14.5629\sigma^3 - 10.8034\sigma^2 - 0.1902\sigma + 1.000 \quad (1.52)$$

In the previous equations, the parameter θ_0 represents the mean orientation angle of the thin dipoles whereas σ accounts for the randomness of the cloud of dipoles.

On the basis of the previous procedure to avoid the extraction of non-physical covariance matrices, *Arii et al.* [R93] proposed an adaptive NNED decomposition theorem, where also the previous extended model for volume scattering is considered. According to the NNED decomposition, a covariance matrix for the volume scattering is first subtracted from the measured covariance matrix as follows

$$\mathbf{C}_{\text{remainder}} = \mathbf{C} - f_v \mathbf{C}_v(\theta_0, \sigma) \quad (1.53)$$

As indicated previously, f_v can be obtained analytically only under the assumption of reflection symmetry. In those cases in which the previous hypothesis does not apply, as proposed in [Ref here], the maximum value of f_v is obtained numerically by calculating the eigenvalues $\mathbf{C}_{\text{remainder}}$ at specific randomness σ and mean orientation angle θ_0 by varying f_v , and then, the maximum f_v in which all three eigenvalues of $\mathbf{C}_{\text{remainder}}$ are nonnegative is selected.

Once the volume component is extracted from the measured covariance matrix as specified in (1.53), the remainder matrix can be written as

$$\mathbf{C} - f_v \mathbf{C}_v(\theta_0, \sigma) = f_d \mathbf{C}_d + f_s \mathbf{C}_s + \mathbf{C}'_{\text{remainder}} \quad (1.54)$$

where in this case \mathbf{C}_d and \mathbf{C}_s correspond to the double-bounce and surface scattering mechanisms already employed in the three-component Freeman-Durden decomposition. The parameters f_d , f_s and $\mathbf{C}'_{\text{remainder}}$ are obtained through an eigenvalue decomposition [Ref here]. This procedure shows how to find the parameters in the decomposition for a specific pair of randomness σ and mean orientation angle θ_0 . To find the best fit decomposition, the power in the remainder matrix for all pairs of randomness and mean orientation angles is evaluated and then find the set of parameters that minimize the power associated with $\mathbf{C}'_{\text{remainder}}$.

Finally, the scattered power at each component $\{f_v, f_d, f_s\}$ may be combined to generate a RGB image similarly as in the case of the Pauli decomposition, to present all the colour-coded polarimetric information in a unique image, see Figure 1.4.

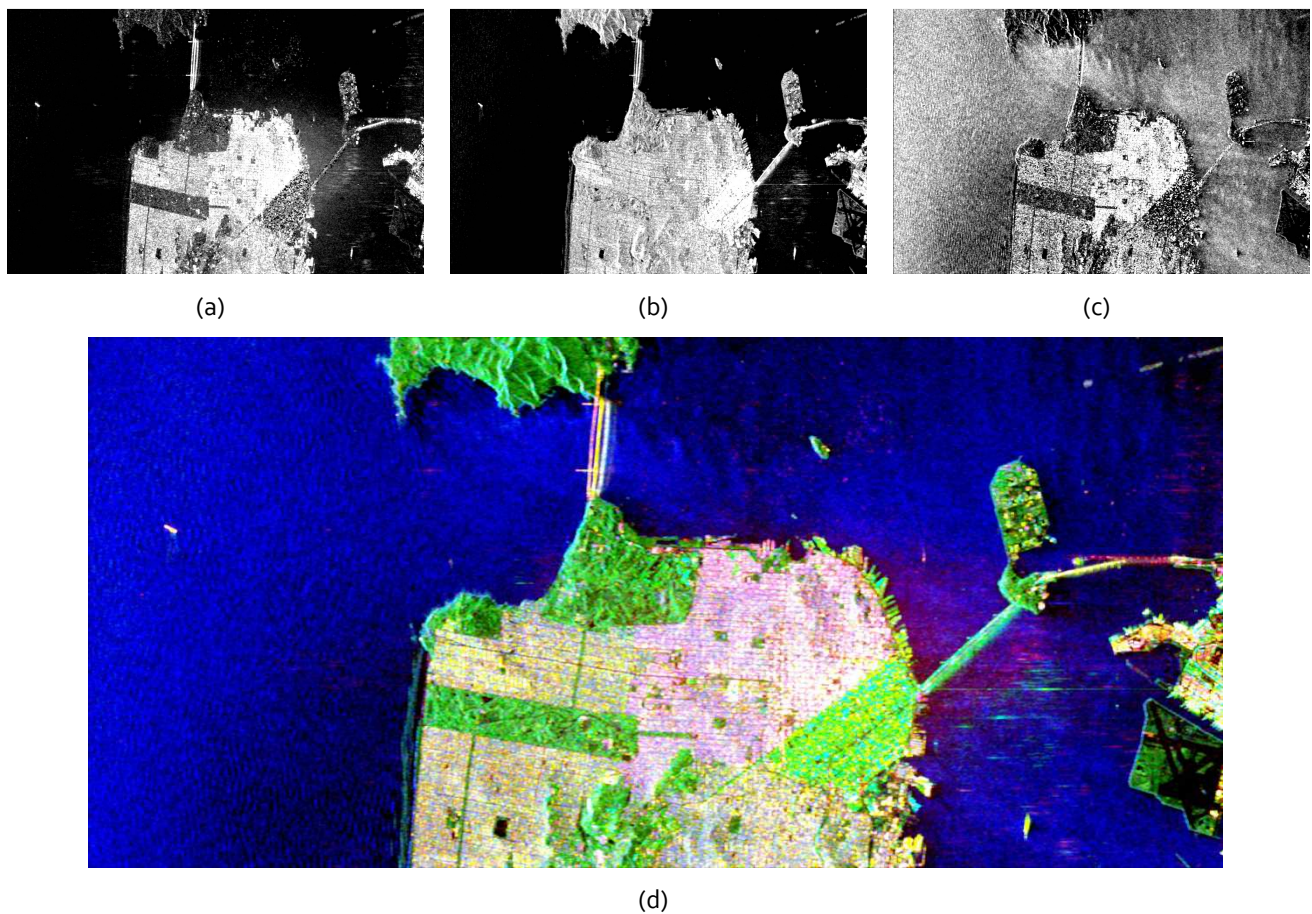


Figure 1.4 – Van Zyl decomposition of the Radarsat-2 polarimetric RGB-Pauli image over San Francisco (USA). (a) f_d , (b) f_v , (c) f_s , (d) RGB composition where f_d red, f_v green and f_s blue.

1.3.5 Eigenvector-Eigenvalue based Decomposition

The previous incoherent decompositions were constructed on the assumption that the scattering of a given pixel was due to the combination of some predefined scattering mechanisms, hence assuming different properties of the scattering processes. These assumptions make these decompositions to be easy to interpret as the different scattering components present a clear physical interpretation. Nevertheless, as these decompositions consider only the predefined mechanisms, they are not able to identify additional scattering mechanisms when present. A way to circumvent this drawback is to decompose the covariance or coherency matrices based on their mathematical properties. Hence, contrarily to the previous decompositions, the scattering mechanisms in which the original matrices are decomposed are not established a priori but given by the decomposition itself. The drawback of this approach is that the scattering mechanism found by the decomposition needs from a physical interpretation process.

The *eigenvector-eigenvalue scattering decomposition*, also known as *Claude-Pottier decomposition*, is based on the eigendecomposition of the covariance \mathbf{C} or coherency \mathbf{T} matrices [R38]. According to the eigendecomposition theorem, the 3×3 Hermitian matrix \mathbf{C} may be decomposed as follows

$$\mathbf{T} = \mathbf{U}\Sigma\mathbf{U}^{-1} \quad (1.55)$$

The 3×3 , real, diagonal matrix Σ contains the eigenvalues of \mathbf{C}

$$\Sigma = \begin{bmatrix} \lambda_1 & 0 & 0 \\ 0 & \lambda_2 & 0 \\ 0 & 0 & \lambda_3 \end{bmatrix} \quad (1.56)$$

such that $\infty > \lambda_1 \geq \lambda_2 \geq \lambda_3 > 0$. The 3×3 unitary matrix \mathbf{U} contains the eigenvectors \mathbf{u}_i for $i = 1, 2, 3$ of \mathbf{C}

$$\mathbf{U} = [\mathbf{u}_1 \ \mathbf{u}_2 \ \mathbf{u}_3] \quad (1.57)$$

The eigenvectors \mathbf{u}_i for $i = 1, 2, 3$ of \mathbf{C} can be reformulated, or parameterized, as

$$\mathbf{u}_i = \begin{bmatrix} \cos \alpha_i & \sin \alpha_i \cos \beta_i e^{j\delta_i} & \sin \alpha_i \cos \beta_i e^{j\gamma_i} \end{bmatrix}^T \quad (1.58)$$

Considering (1.55), (1.56) and (1.57), the coherency matrix \mathbf{C} may be written as

$$\mathbf{C} = \sum_{i=1}^3 \lambda_i \mathbf{u}_i \mathbf{u}_i^{*T} \quad (1.59)$$

As (1.59) shows, the rank 3 matrix \mathbf{C} can be decomposed as the combination of three rank 1 coherency matrices formed as

$$\mathbf{C}_i = \mathbf{u}_i \mathbf{u}_i^{*T} \quad (1.60)$$

which can be related to the pure scattering mechanisms given in (1.58). Consequently, the eigendecomposition is not able to produce scattering mechanisms in which the original matrix is decomposed into with a rank larger than 1.

The eigenvalues (1.56) and the eigenvectors (1.57) of the decomposition are considered as the primary parameters of the eigendecomposition of \mathbf{C} . In order to simplify the analysis of the physical information provided by this eigendecomposition, three secondary parameters are defined as a function of the eigenvalues and the eigenvectors of \mathbf{C}

- *Entropy*

$$H = - \sum_{i=1}^3 p_i \log_3(p_i) \quad p_i = \frac{\lambda_i}{\sum_{j=1}^3 \lambda_j} \quad (1.61)$$

where p_i are known as the probabilities of the eigenvalue λ_i , respectively. These probabilities represent the relative importance of this eigenvalue respect to the total scattered power, as

$$SPAN(\mathbf{S}) = |S_{hh}|^2 + |S_{vv}|^2 + 2|S_{hv}|^2 = \sum_{i=1}^3 \lambda_i \quad (1.62)$$

- *Anisotropy*

$$A = \frac{\lambda_2 - \lambda_3}{\lambda_2 + \lambda_3} \quad (1.63)$$

representing the relative importance of the second eigenvalue with respect to the third one.

- *Mean alpha angle*

$$\bar{\alpha} = \sum_{i=1}^3 p_i \alpha_i \quad (1.64)$$

As it shall be shown, this parameter allows the physical interpretation of the scattering mechanism found by the eigendecomposition.

The eigen decomposition of the coherency matrix is usually referred to as the $H/A/\bar{\alpha}$ decomposition. The interpretation of the information provided by the eigendecomposition of the coherency matrix must be performed in terms of the eigenvalues and eigenvectors of the decomposition or in terms of $H/A/\bar{\alpha}$. Nevertheless, both interpretations have to be considered as complementary.

The interpretation of the scattering mechanisms given by the eigenvectors of the decomposition, \mathbf{u}_i for $i = 1, 2, 3$, is performed by means of a mean dominant mechanism which can be defined as follows

$$\mathbf{u}_0 = \begin{bmatrix} \cos \bar{\alpha} & \sin \bar{\alpha} \cos \bar{\beta} e^{j\bar{\delta}} & \sin \bar{\alpha} \cos \bar{\beta} e^{j\bar{\gamma}} \end{bmatrix}^T \quad (1.65)$$

where the remaining average angles are defined in the same way as $\bar{\alpha}$

$$\bar{\beta} = \sum_{i=1}^3 p_i \beta_i \quad \bar{\delta} = \sum_{i=1}^3 p_i \delta_i \quad \bar{\gamma} = \sum_{i=1}^3 p_i \gamma_i \quad (1.66)$$

The mean magnitude of the mechanism is obtained as

$$\bar{\lambda} = \sum_{i=1}^3 p_i \lambda_i \quad (1.67)$$

The study of the mechanism given in (1.65) is mainly performed through the interpretation of the mean alpha angle $\bar{\alpha}$, since its value can be easily related with the physics behind the scattering process. The next list details the interpretation of $\bar{\alpha}$:

- $\bar{\alpha} \rightarrow 0$: The scattering corresponds to single-bounce scattering produced by a rough surface.
- $\bar{\alpha} \rightarrow \pi/4$: The scattering mechanism corresponds to volume scattering.
- $\bar{\alpha} \rightarrow \pi/2$: The scattering mechanism is due to double-bounce scattering.

The second part in the interpretation of the eigendecomposition is performed by studying the value of the eigenvalues of the decomposition. A given eigenvalue corresponds to the associated scattered power to the corresponding eigenvector. Consequently, the value of the eigenvalue gives the importance of the corresponding eigenvector or scattering mechanism. The ensemble of scattering mechanisms is studied by means of the Entropy H and the Anisotropy A. The Entropy H determines the degree of randomness of the scattering process, which can be also interpreted as the degree of statistical disorder. In this way:

- $H \rightarrow 0$:

$$\lambda_1 = SPAN \quad \lambda_2 = 0 \quad \lambda_3 = 0 \quad (1.68)$$

As observed, in this case, the coherency matrix \mathbf{T} presents rank 1 and the scattering process corresponds to a pure target.

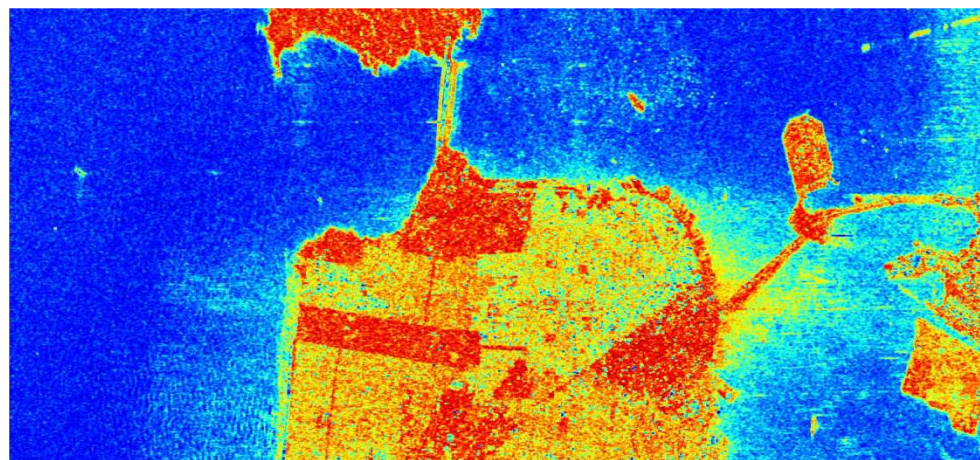
- $H \rightarrow 1$:

$$\lambda_1 = \frac{SPAN}{3} \quad \lambda_2 = \frac{SPAN}{3} \quad \lambda_3 = \frac{SPAN}{3} \quad (1.69)$$

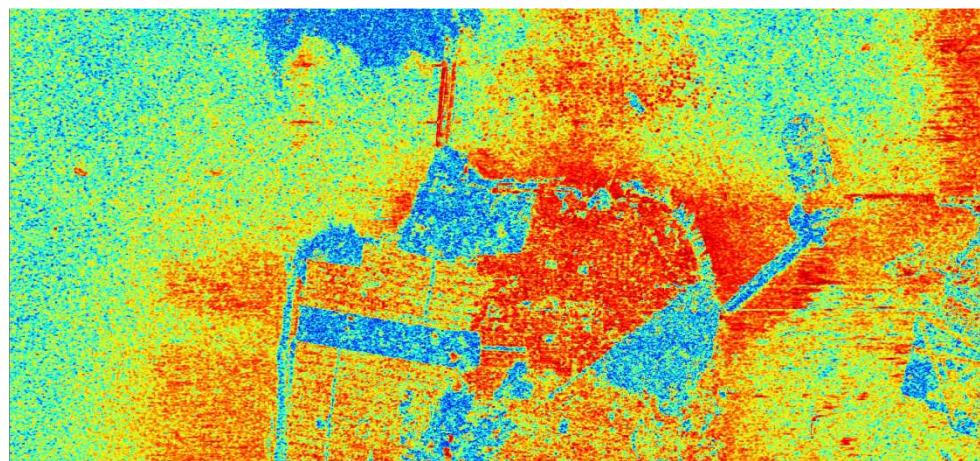
In this situation, the scattering matrix \mathbf{C} presents rank 3, that is, the scattering process is due to the combination of three pure targets. Consequently, \mathbf{C} corresponds to the response of a distributed target. For instance, volume scattering for a forest canopy presents an Entropy value very close to one.

- $1 > H > 0$: In this case, the final scattering mechanism given by \mathbf{C} results from the combination of the three pure targets given by \mathbf{u}_i for $i = 1, 2, 3$, but weighted by the corresponding eigenvalue.

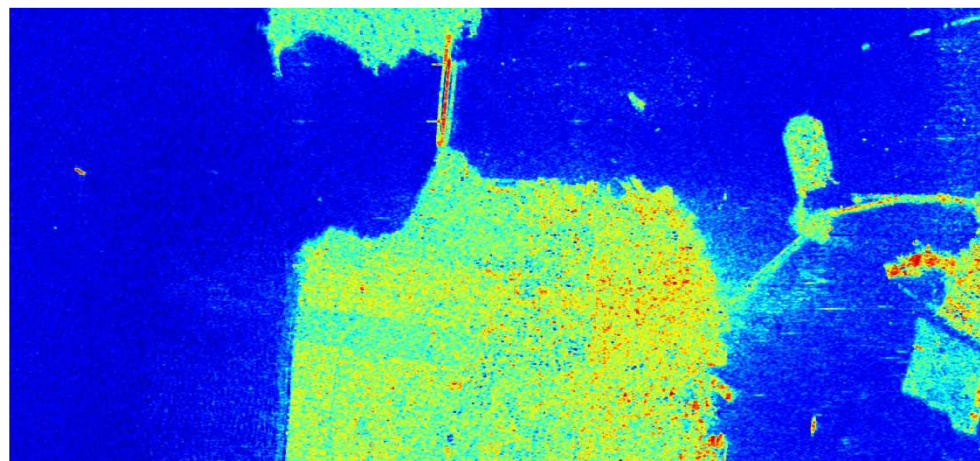
The Anisotropy A, (1.63), is a parameter complementary to the Entropy. The Anisotropy measures the relative importance of the second and the third eigenvalues of the eigendecomposition. From a practical point of view, the Anisotropy can be employed as a source of discrimination only when $H > 0.7$. The reason is that for lower entropies, the second and third eigenvalues are highly affected by the SAR system noise.



(a)



(b)



(c)

Figure 1.5 – $H / A / \bar{\alpha}$ decomposition of the Radarsat-2 polarimetric RGB-Pauli image over San Francisco (USA).
(a) Entropy, (b) Anisotropy, (c) Mean alpha angle.

In relation with the previous parameters, the Shannon Entropy (SE) was introduced in [R39]

$$SE = \log(\pi^3 e^3 |\mathbf{T}|) = SE_I + SE_P \quad (1.70)$$

as the sum of two terms. The term SE_I is the intensity contribution that depends on the total power

$$SE_I = 3 \log\left(\frac{\pi e I}{3}\right) = 3 \log\left(\frac{\pi e \text{Tr}(\mathbf{T})}{3}\right) \quad (1.71)$$

whereas SE_P is the polarimetric contribution

$$SE_P = \log\left(27 \frac{|\mathbf{T}|}{\text{Tr}^3(\mathbf{T})}\right) \quad (1.72)$$

As indicated previously, for some particular configurations, a polarimetric SAR system may not measure the complete polarimetric information. In this simpler configuration of dual polarization, the radar transmits only a single polarization and receives, either coherently or incoherently, two orthogonal components of the scattered signal. In this configuration, the covariance \mathbf{C} and coherency \mathbf{T} matrices are 2×2 Hermitian matrices. As it has been demonstrated previously, these reduced matrices can be decomposed also consider their eigendecompositions. The sole particularity is that since in this situation, the matrices present only two eigenvalues, the Entropy and Anisotropy parameters represent the same information.

1.3.6 The Touzi target scattering decomposition

The Touzi decomposition [R40][R41] was introduced as an extension of the Kennaugh-Huynen coherent target scattering decomposition (CTD) [R42][R8] for the characterization of both coherent and partially coherent target scattering. To characterize partially coherent scattering, Huynen introduced a target decomposition theorem in which he decomposed an average Mueller matrix into the sum of a Mueller matrix for a single scatter, presented in terms of the Kennaugh-Huynen CTD parameters and a noise the N-target Mueller matrix [R8]. In 1988, Cloude [R43] has showed that the Huynen N-target decomposition was not polarization independent, and introduced the eigen vector decomposition for a unique and roll invariant ICTD. Following that, both Huynen's (N-target) ICTD and Huynen's fork CTD were abandoned. Recently, the Kennaugh-Huynen CTD has been reconsidered and integrated it in Cloude's coherency eigen vector decomposition [R43] for characterization of coherent and partially coherent scattering in terms of unique and polarization basis independent parameters [R40][R41].

The Kennaugh-Huynen CTD, also named the Huynen fork, used to be the most popular method for decomposition of coherent target scattering [R44][R45]. Huynen's fork was abandoned because of the nonuniqueness of certain fork parameters, and in particular the skip angle (scattering type phase), due to nonuniqueness of the con-eigenvalue phases [R46]. To solve for these ambiguities, the Kennaugh-Huynen scattering matrix con-diagonalization was projected into the Pauli basis [R40], and a new Target Scattering Vector Model, the TSVM, was introduced in terms of target parameters that are not affected by the con-eigenvalue phase ambiguities [R40][R41]. A complex entity, named the symmetric scattering type, was introduced for an unambiguous description of target scattering type. The polar coordinates of the symmetric scattering type, α_s and ϕ_{α_s} , were expressed as a function of target scattering matrix polarization basis independent elements by [R40][R41]

$$\tan \alpha_s \cdot e^{j\phi_{\alpha_s}} = \frac{\mu_1 - \mu_2}{\mu_1 + \mu_2} \quad (1.73)$$

where μ_1 and μ_2 are the con-eigenvalues of the target scattering matrix \mathbf{S} . The scattering vector of a symmetric scatterer can be expressed on the Pauli trihedral-dihedral basis $\{\mathbf{S}_a, \mathbf{S}_b\}$ as follows [R40][R41]

$$\vec{V}_{sym} = |\vec{V}_{sym}| \cdot [\cos \alpha_s \cdot \mathbf{S}_a + \sin \alpha_s \cdot e^{j\phi_{as}} \mathbf{S}_b] \quad (1.74)$$

where the scattering type magnitude α_s corresponds to the orientation angle of the symmetric scattering vector on the trihedral-dihedral $\{\mathbf{S}_a, \mathbf{S}_b\}$ basis. ϕ_{as} is the phase difference between the vector components in the trihedral-dihedral basis. The new scattering type phase entity introduced in [R40] provides a measure of the phase offset between the trihedral and dihedral scattering components. The information provided by ϕ_{as} as complementary to α_s was shown to be essential for a better understanding of marsh wetland scattering variations between the spring run off season and the fall using Convair 580 SAR data collected over the Mer Bleue wetland site[R41][R47]. The symmetric and asymmetric nature of target scattering was characterized using Huynen helicity τ [R40]. Notice that while the complex scattering parameters α_s and ϕ_{as} are independent of the basis of polarization [R40][R48], Huynen's helicity characterizes the symmetric nature of target scattering in the $\{h, v\}$ polarization basis [R8]. Recently, a different expression of the helicity was derived at the circular polarization basis [R8], and the complementary information it provides to the Huynen's helicity was demonstrated [R48].

The projection of the Kennaugh-Huynen CTD on the Pauli's polarization basis can be represented as a function of the complex scattering α_s and ϕ_{as} and the Huynen maximum polarization parameters ψ , and m , as [R40][R41]

$$k = m \begin{bmatrix} 1 & 0 & 0 \\ 0 & \cos 2\psi & -\sin 2\psi \\ 0 & \sin 2\psi & \cos 2\psi \end{bmatrix} \begin{bmatrix} \cos \alpha_s \cos 2\tau \\ \sin \alpha_s e^{j\phi_{as}} \\ -j \cos \alpha_s \sin 2\tau \end{bmatrix} \quad (1.75)$$

where ψ , τ and m are the Huynen orientation, the helicity and the maximum return of the maximum polarization, respectively.

It is worth noting that for a symmetric scattering ($\tau=0$), α_s and ϕ_{as} are identical to the Touzi SSCM [R86] parameters η and $\phi_{Sb} - \phi_{Sa}$, which were shown to be promising for ship identification [R86]. α_s and ϕ_{as} are also identical to the Cloude-Pottier parameters [R38] α and $\delta = \phi_2 - \phi_1$, respectively [R40]. For targets of locally asymmetric scattering, such as urban areas, treed wetlands and forests, large divergence between ϕ_{as} and δ , and α_s and α have been noted [R40][R41]. Unlike Cloude-Pottier parameters [R38], the TSVM characterizes target scattering type with the complex entity (α_s and ϕ_{as}), which only depends on the scattering matrix eigenvalues. This leads to a unique and unambiguous description of target scattering in terms of parameters, which are polarization basis independent, for both symmetric and asymmetric targets as discussed in [R40][R41].

For a unique characterization of coherent and partially coherent scattering, the TSVM [R40] was integrated in Cloude's coherency eigen vector decomposition [R26]. Like Wiener's wave coherence characteristic decomposition [R49], Cloude's characteristic decomposition of the coherency matrix, \mathbf{T} , permits the representation of \mathbf{T} as the incoherent sum of coherency matrices that represent independent single scattering [R43]. Under the target reciprocity assumption, \mathbf{T} is represented as the sum of up to three coherency matrices \mathbf{T}_i , each of them being weighted by its appropriate positive real eigenvalue η_i :

$$\mathbf{T} = \sum_{i=1,2,3} \eta_i \mathbf{T}_i \quad (1.76)$$

In contrast to the Cloude-Pottier decomposition [R38], the TSVM is used for the parameterization of each coherency eigenvector \mathbf{T}_i (coherent single scattering) in terms of unique target parameters. In order to avoid any loss of information related to single scatterer parameters averaging, the target scattering decomposition is conducted through an in-depth analysis of each of the three single scattering eigenvectors i ($i=1,3$) represented by the coherency eigenvector matrix \mathbf{T}_i of rank 1 and the normalized positive real eigenvalues $\lambda_i = \eta_i / (\eta_1 + \eta_2 + \eta_3)$. This leads to the representation of each single scattering i in terms of five roll invariant and independent target scattering parameters: $(\alpha_{si}, \phi_{\alpha si}, \tau_i, m_i, \lambda_i)$ and the Huynen orientation angle ψ_i .